The Thesis Committee for Andre Matthew Williams
Certifies that this is the approved version of the following thesis:

Determining the molecular underpinnings of extracellular matrix breakdown during choroid fissure closure

APPROVED BY
SUPERVISING COMMITTEE:

Supervisor:

Jeffrey Gross

John Wallingford

Determining the molecular underpinnings of extracellular matrix breakdown during choroid fissure closure

by

Andre Matthew Williams, B.A

Thesis

Presented to the Faculty of the Graduate School of

The University of Texas at Austin

in Partial Fulfillment

of the Requirements

for the Degree of

Master of Arts

The University of Texas at Austin

May 2016

Dedication

I dedicate this thesis to my grandparents, Gordon and Patricia, who saw potential in me when I was young, and have been a guiding light during this process. I dedicate this to my mother, who has given so much of her time, effort, and love to nurture me and my aspirations. I dedicate this to my fathers, Andre and Rodney, who both have set me on a path to become the man I am today. I dedicate this to my friends, who help me keep my sanity and are always willing to listen. And I dedicate this to my family, who never fails to tell me how proud they are at every chance.

Acknowledgements

I would like to thank Dr. Jeffrey Gross for helping me formulate ideas, design experiments and critical reading of this thesis. I would like to thank Dr. Seema Agarwala for allowing me to perform experiments using chicken in her lab. I would like to thank Dr. John Wallingford for critical reading of this thesis.

I would like to thank Dr. Emily McMains and Nicholas Hanovice for guiding me through the writing process. I would like to thank the remaining members of the Gross lab, Pawat Seratrukil, Dr. Andrea Hartsock, Krista Angileri, Kristen Koenig, and Natalie Gath, for advice and support while drafting this thesis. I would like to thank Ryoko Minowa for keeping our fish facility running. Finally, I would like to thank Dr. Nicolas Hirsch for supporting me since my undergraduate career.

Abstract

Determining the molecular underpinnings of ECM breakdown during choroid fissure closure

Andre Matthew Williams, M.A.

The University of Texas at Austin, 2015

Supervisor: Jeffrey Gross

Proper closure of the choroid fissure (CF), a transient structure present during early eye development, is critical for eye organogenesis. Choroid fissure closure (CFC) is a dynamic process that requires morphogenetic movements, extracellular matrix (ECM) breakdown, and tissue fusion. Defects in this process result in coloboma, which is responsible for 3-11% of childhood blindness worldwide. Little is known about the mechanism of ECM breakdown during CFC, or what tissues are responsible for facilitating it. We hypothesized that podosomes, small actin-based structures that are capable of breaking down ECM in other cellular contexts, are responsible for ECM breakdown during CFC. Using a mutant of the actin-linker protein Talin, we show that Talin is not responsible for ECM breakdown, as normal ECM breakdown occurs in *talin*^{HI3093Tg} mutants. Mutation of *tks4*, a core podosome component, results in a small coloboma, suggesting a likely role for podosomes in proper retinal fusion. Previous data suggested that the hyaloid vasculature, which passes through the CF to envelop the lens,

is involved in degrading the ECM during CFC. Though the hyaloid vasculature is present, Actin within the hyaloid vasculature did not localize to regions that have intact ECM, suggesting that the hyaloid vasculature is not involved in ECM breakdown. Finally, I used chicken as a potential new model organism to investigate mechanisms of breakdown in CFC. However, no ECM breakdown was observed in chicken CFC, and invasion of mesenchymal cells that separates the CF was observed. Further investigation is required to determine the molecular underpinnings of CFC.

Table of Contents

List of Figures

Introduction

Vision is a critical part of the way many organisms experience the environment. The ability to perceive movement, shapes, and colors is crucial for both food acquisition and threat avoidance. During vertebrate development, the eyes begin as protrusions of tissue, termed the optic vesicles[1], from the diencephalon,. The optic vesicles extend outward to the surface ectoderm, and invaginate to form the optic cups, composed of neural retina and retinal pigment epithelium (RPE). During invagination, the developing optic cup has a ventral opening, the choroid fissure, which allows for the entry of the vasculature and exit of the optic nerve. As eye development progresses, the choroid fissure meets and the two edges fuse to become a continuous optic cup. This process, called choroid fissure closure (CFC), consists of three major phases: (1) apposition of the two edges of the choroid fissure, (2) breakdown of the extracellular membrane (ECM) along the edges of the fissure, and (3) fusion of the choroid fissure. Failure of CFC results in a gap in the ventral hemisphere of the eye called a coloboma. Colobomas vary in severity depending on where CFC failure occurs[2,3]. Coloboma occurs in 3-11% of cases of blindness worldwide[4], and even without causing blindness, coloboma can greatly affect visual acuity[5,6]. However, less than 20% of patients with coloboma have an identified genetic cause that underlies the defect [3,4,7]. Understanding the genetic and cell biological underpinnings of CFC will aid in understanding coloboma and will elucidate morphogenetic processes driving this important developmental event.

Zebrafish are an ideal model system in which to study CFC due to their small size, large egg clutches, and rapid external development. There are a number of tools that exist for zebrafish that allow for simple yet powerful genetic manipulations to effect developmental processes. Zebrafish embryos are transparent, making live-imaging experiments of morphogenetic events

simple. A high degree of anatomical similarity between human and zebrafish eyes allow comparisons between the two[8]. Likewise, eye development is very similar in the two species. In zebrafish embryos, the choroid fissure becomes apparent at the 18 somite stage[1] at 18 hours post fertilization (hpf), lasting until about 60 hpf (unpublished results). The early onset and rapidity of eye organogenesis in zebrafish allows for live imaging of choroid fissure closure *in toto*. What we learn about CFC in zebrafish will be highly relevant for understanding the dynamics of CFC in humans.

This thesis focuses on the second phase of CFC, in which the ECM that surrounds the edges of the CF is degraded prior to fusion. To understand the cellular mechanisms driving this phase, we need to understand what factors regulate ECM breakdown. Failure of ECM breakdown has been correlated with coloboma in a number of organisms, suggesting ECM breakdown is required for CFC to occur. Experiments in mice show that at points of fusion within the choroid fissure, cellular processes extend across the fissure and the basement membrane is absent from these regions[9–11]. In mice who have a condition called Fatty liver shinogi (FLS), the basement membrane persists and prevents the two edges of the retina from fusing, resulting in coloboma[12]. Disruption of *pax2* in chick and *Xenopus* results in a failure of ECM breakdown and coloboma[13–15]. Though ECM breakdown seems to be critical for CFC, the cell biological mechanism through which breakdown is achieved has yet to be discovered. Previous work from our lab has identified the timeframe during which ECM breakdown occurs in zebrafish. ECM breakdown begins after the two edges of the retina become apposed, between 31 and 34 hpf. By exploring the developmental processes that facilitate CFC, I aim to uncover how the ECM is degraded during CFC.

To understand the molecular processes that facilitate ECM breakdown during CFC, a mechanism that is capable of degrading the ECM in the choroid fissure needs to be identified. As actin is present at sites of degradation within the CF, we investigated a mechanism that utilizes actin to facilitate ECM degradation. Podosomes are structures we hypothesize could be involved in ECM breakdown during CFC, as they are actin-based protrusions of the cellular membrane that are able to degrade the ECM in a number of cellular contexts[16,17]. Podosomes have been observed in a number of *in vitro* systems, including osteoclast cultures[18], microglia[19] and tumor cells[20]. A well studied developmental event in which podosomes are shown to be required is anchor cell invasion of the vulva of *C. elegans*[21,22]. Podosomes have also been investigated *in vivo* in *Xenopus* during neural crest cell migration[23], and in the growth cones of axons within the spinal cord [24]. To determine if podosomes are required for ECM breakdown during CFC, I utilized mutants of core genes necessary for the formation of podosomes.

Tks4, also known as Sh3pxd2b, is required within podosomes for their proper function[25,26]. In addition, Tks4 also recruits matrix metalloproteases (MMPs) to the cell surface to degrade the ECM[26–29]. *In situ* hybridization shows that *tks4, mmp14a,* and *mmp2* are present within the choroid fissure, giving further support for a model in which podosomes could be involved in CFC (Chanjae Lee, unpublished results) Thus, to test the hypothesis that podosomes are involved in ECM breakdown in the choroid fissure, we created a *tks4* mutant line through targeted mutagenesis using TALEN[30,31].

Talin is a linker protein that connects filamentous actin (F-Actin) to proteins such as Integrin that interact with the ECM[32–34]. This is critical for the cell to sense its environment. Talin serves as a mechanosensor, where tension on the actin skeleton allows for orientation of the cell in space (reviewed in [35,36]). Talin is also enriched in focal adhesions that contain Tks5, a

second protein critical for podosome formation[37]. Previous data from our lab demonstrate that the *talin*^{HI3093Tg} mutant line has coloboma. We have also observed through immunohistochemical assays that the ECM has not been degraded in the CF of these mutants. As Talin is shown to be a component of podosomes, we hypothesized that Talin could be involved in podosome-mediated ECM degradation in the choroid fissure.

Our preliminary data support a model in which podosomes are responsible for ECM breakdown within the CF; however, the cell type responsible for breaking down the ECM has yet to be discovered. Preliminary evidence suggests that the hyaloid vasculature may in fact be this cell type. The hyaloid vasculature enters the retina through the choroid fissure, and is responsible for supplying nutrients to the developing lens[38]. In zebrafish, the hyaloid vasculature enters the retina at about 19hpf, and persists within the fissure throughout CFC[39]. As the hyaloid vasculature is present within the fissure directly preceding closure, we investigated whether the vasculature facilitates ECM breakdown. Hyaloid vasculature is made up of endothelial sells, which have been shown to have podosomes to facilitate angiogenesis[40–42]. As such, the hyaloid vasculature should be investigated for the potential to degrade the ECM. Previous data have also shown concentrations of actin within the hyaloid vasculature that localize with regions of ECM breakdown during CFC. Projections from the vasculature have also been observed that seem to extend within the CF, which we speculate could be podosomes extending into the retina, as they appear near the site of fusion.

To gain a complete understanding of the molecular players driving ECM breakdown during CFC, the ability to scrutinize many individual proteins specifically involved in actin-mediated degradation is required. Creating stable, targeted mutant lines in zebrafish is time consuming and labor intensive. Embryos with targeted genetic ablations must be raised to sexual

maturity and multiple alleles screened. A more efficient approach would be to conditionally express altered candidate proteins in just the CF. Transient, spatially targeted expression of dominant negative and constitutively active versions of proteins is a well-established approach in chicken. Previous work in other labs has shown that cell dynamics within the neural tube can be studied using explantation of chicken embryos (Brown, C, Agarwala, S. unpublished results). Electroporation of DN and CA constructs allow for an internal control, as electroporation can be spatially targeted[43,44]. Chicken embryos have much larger eyes than zebrafish, making explanting eye tissue feasible. Therefore, we investigated CFC in the chicken in order to evaluate its appropriateness as a model organism for CFC that would allow us to explore the role of specific genes in ECM breakdown.

Methods

Immunohistochemistry.

Embryos were collected 15 minutes after breeding began. Embryos were kept @ 28.5°C in fish water until proper age for study. Embryos were fixed in 4% paraformaldehyde in 1x phosphate buffered saline (PBS) overnight. Fish were washed for 5 minutes 3 times in PBS. Fish were cryoprotected by submerging in 25% and 35% sucrose in PBS. Fish were then mounted using Tissue Freezing Medium (TFM) (Triangle Biomedical Science, Durham, NC) and frozen at -80°C. Sectioning was performed on a Microm HM 550 cryostat (Thermofisher, Waltham, MA) at -20°C using Thermofisher Superfrost + II slides. Slides were kept at 4°C after sectioning. Staining protocol as described previously (Gross & Uribe 2007) Antibodies: mouse polyclonal anti-GFP (SC9996, Santa Cruz Biotechnology, Dallas, TX, USA), 1:100; rabbit polyclonal anti-laminin (Sigma, #L9393), 1:200; Phalloidin (AlexaFluor 555 or 633, Invitrogen, Waltham, MA, USA), 1:33; DAPI (D9542, Sigma, St. Louis, MO, USA), 1:250.

Imaging

Embryos were collected 15 minutes after fertilization and kept @ 28.5°C in fish medium until proper age for study. Embryos were de-chorionated by using forceps and anesthetized using MS-200 (Tricane). Embryos were oriented on their side in 1% agarose for imaging the sagittal plane and submerged in 10% Tricane in fish water to ensure anesthetization of embryos through imaging. All images were taken on a Leica TCS SP5 II equipped with a 25x immersion objective. Following imaging, embryos were freed from the agarose and placed in a petri dish for further analysis. Bright field images were captured using a Leica MZ16F stereomicroscope mounted with a DFC480 digital camera (Leica, Mannheim, Germany).

Genotyping

D. Rerio AB strain embryos were injected with TALEN constructs for tks4. Embryos were grown to 3-6 months before genotyping. DNA was obtained from tail fin clips dissolved in 100mM Sodium hydroxide at 95°C. Samples were neutralized with 0.5 M Tris-HCl at pH 8.0. Primers: tks4 Forward 5'-gttcgcttggtccagactgcag3' Reverse 5'-cctcctgatcacatctccagcctc-3' Talin^{Hi3903} : 5'-taccagcatttactcaacaggaac-3' and 5'-ccaaacctacaggtggggtc-3'.

Screening of TALEN mutants

TALEN constructs were created using the Golden Gate protocol[45]. TALENS were designed to the *tks4* locus with a 15 bp Spacer: Forward strand 5' – tactagaagtaact – 3' Reverse strand 5' – tggggtttcttctctt – 3'. Embryos were injected with TALEN mRNA at the 1-4 cell stage. F0 founders were screened for frameshift mutations using Restriction Fragment Length Polymorphism (RFLP). Enzyme: BmgB1 (New England Biolabs, Ipswich, MA, USA) used for 3 hours at 37°. Sanger sequencing using Applied Biosystems was completed at the University of Texas at Austin Institute of Cellular and Molecular Biology (ICMB). All cloning performed for genotyping was completed with pGEM according to protocol (Promega, Madison, WI, USA). DH5α competent cells were used in all experiments unless otherwise noted (New England Biolabs Ipswich, MA, USA). All plates were incubated at 37°C for 14-18 hours. Colonies were grown in 3mL of LB broth with 100mg/mL of ampicillin. DNA extraction was carried out using the QIAgen Miniprep kit (QIAgen, Venlo, Limburg, Germany).

Animals

Zebrafish were maintained in our facilities as described (Westerfield, 1995). Embryos were obtained and staged as described in (Kimmel et al., 1995). Transgenics used were Tg(*kdrl:moesinGFP*) and Tg(*kdrl:mCherry*) transgenic lines [46]. *Talin*^{HI3093tg} was obtained from ZIRC (Eugene, OR, USA). All protocols used within this study were approved by the Institutional Animal Care and Use Committee of The University of Texas at Austin and conform to the National Institutes of Health Guide for the Care and Use of Laboratory Animals. Fertilized Leghorn eggs (Texas A&M Poultry Science Center) were incubated at 38°C and staged according to Hamburger and Hamilton [47]. Chicken embryos were collected at E3, E4, and E4.5.

Results

Figure 1. Mild *talin*^{Hi3093Tg} mutants show normal ECM breakdown. (A)*talin*^{HI3093Tg} mutants lack laminin staining at 2 dpf, suggesting ECM breakdown has occurred in these embryos. (B)The phenotype is the same for *talin*^{HI3093Tg} sibling embryos. (C,D) No laminin staining can be seen at 3 dpf, suggesting ECM breakdown has occurred normally in these embryos.

Figure 2. *tks4* mutant does not have a visible phenotype. (A). Gene region obtained from Ensembl (http://useast.ensembl.org/index.html) showing mutation targeted to first exon (red bar). (B) Nucleotide sequence showing location of nonsense mutation within the tks4 locus (red box). Arrows show transcription start site, arrowheads show end of the first exon (A,B) Protein sequence displays two early stop codons at the C-terminus of the peptide (B, black asterisks), resulting in a truncated form of Tks4. Both sibling (C) and *tks4*$^{-/-}$ mutant (D) embryos present with normal external eye development at 3 dpf.

Figure 3. *tks4* mutants mild coloboma. Wildtype *tks4* siblings (A,B) shows normal lamination within the retina, with full closure of the choroid fissure. Nuclei are marked with DAPI, and phalloidin marks F-actin. The *tks4* mutant (C,D) shows a region of the retina that presents with a gap in the retina and concentration of actin, with higher resolution images in (F, G). E shows orientation of fish embryos. Scale bar =20μm

Figure 4. Live imaging of wildtype hyaloid vasculature show vascular extensions on ventral surface of optic cup. Time lapse live imaging of Tg(*kdrl:mCherry)* used to mark hyaloid vasculature membrane does not show protrusions during choroid fissure closure (red = Tg(*kdrl:mCherry)*). Vascular extensions move along the ventral surface of the optic cup, which connect and create another lumen (white arrowheads). However, no projections can be seen extending from the vasculature that would indicate podosomes. Fish cartoon shows orientation of images Scale bar = 10 μm.

Figure 5. Live imaging of *talin*^{HI3093} mutant hyaloid vasculature shows collapsed lumen and no vascular extensions. *talin*^{HI3093} mutant embryos show a collapsed lumen with little to no movement of hyaloid vascular cells within the choroid fissure (red = Tg(*kdrl:mCherry)*). Very few cellular extension can be seen, which fail to make connection like the wildtype sibling (white arrowhead). Fish cartoon shows orientation of images. Scale bar = 10 μm.

Figure 6. Hyaloid vasculature cells are not present in choroid fissure during basement membrane breakdown. (A, E, I). Phalloidin stains actin in both hyaloid vasculature and retinal cells. At 32hpf, the basement membrane extends the full length of the CF (A, bracket), but by 34hpf (E and I), the absence of laminin in the center of the dorsal-ventral axis indicates that the basement membrane in that area has been degraded. (B, F, J) Laminin antibody labeling of sagittal sections through the central portion of the eye reveal the presence of a basement membrane at the edges of the choroid fissure. (C, G, K) Tg(kdrl:moesinGFP) expression shows actin within vasculature cells. The persistence of laminin in CF regions lacking GFP signal at 36hpf (L, arrow) suggests that basement membrane breakdown is not mediated by actin in vasculature cells. Presence of phalloidin stain in the CF in the absence of laminin expression suggests that basement membrane breakdown is an actin dependent process.

Figure 7. Mesenchymal cells invade chicken choroid fissure during timeframe of closure. (A) At HH16, choroid fissure is closing, but is not apposed. (B, D) HH18 shows tight apposition of the choroid fissure with no gaps between the two leading edges of the retina. The red box in (B) denotes area in (D). Red arrow points to tight apposition of the two edges of the retina at HH18. (C, E) HH22 shows invasion of mesenchymal cells within the choroid fissure. Red box in (C) outlines area in (E). Red arrow points to mesenchymal cells residing within the choroid fissure with no fusion of the two leading edges of the retina.

Figure 8. Immunohistochemistry of chicken choroid fissure shows no breakdown of ECM during invasion of mesenchymal cells. (A) HH18 embryos have tight apposition of the edges of the retina, with mesenchymal cells seen within the fissure (yellow arrow). (B) HH21 embryos have no breakdown of laminin (green) within the choroid fissure, and mesenchymal cells separate the leading edges of the retina. (D) Tight apposition of the two edges of the retina, but no basement membrane breakdown is apparent, as laminin signal is intact. (F) The edges of the choroid fissure separate again, with mesenchymal cells residing within the gap of the retina. (C) Mesenchymal cells (blue) invade the choroid fissure and separate the two edges of the retina at HH23, with laminin signal present suggesting no breakdown of ECM. (E)As seen before, the medial portion of the choroid fissure is tightly apposed, but no breakdown of laminin is present at HH23. (G) The retina again separates towards the proximal region of the eye, with mesenchymal cells present within the fissure. Scale bar =50μm

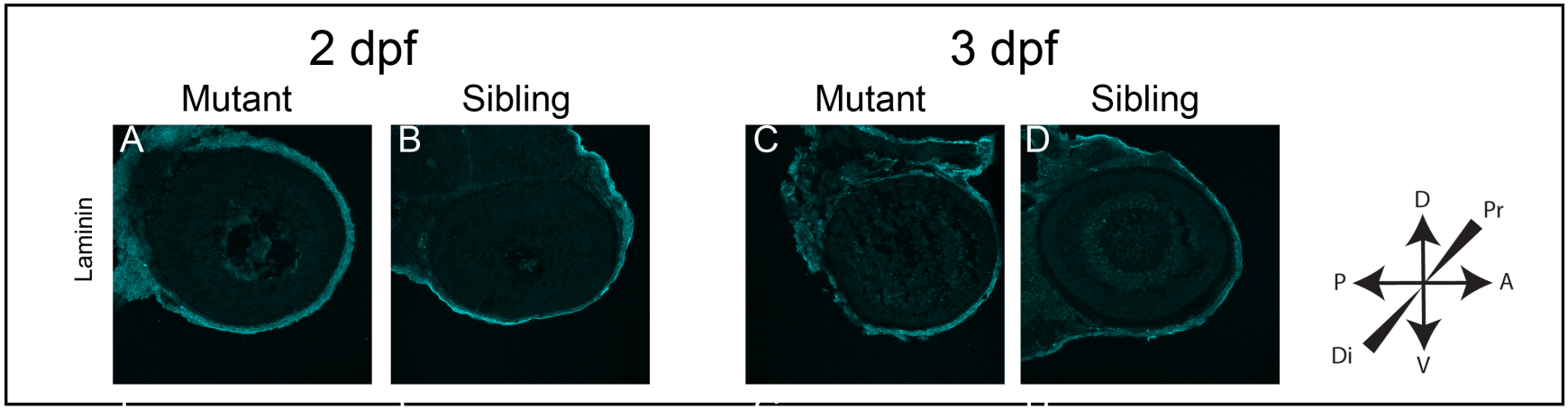

Figure 1: Mild *talin*^{Hi3093Tg} mutants show normal ECM breakdown

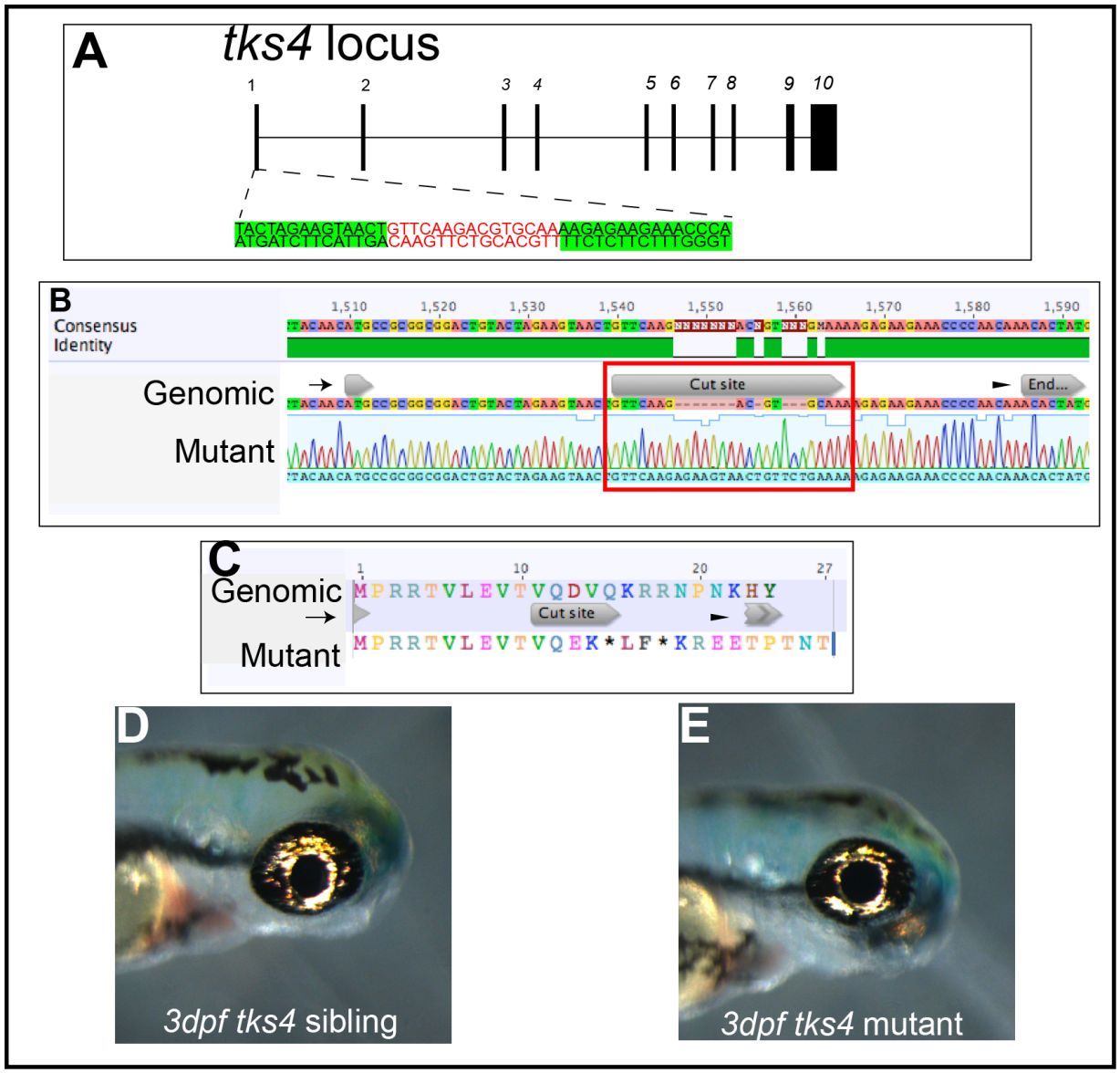

Figure 2: *tks4* mutant does not have a visible phenotype

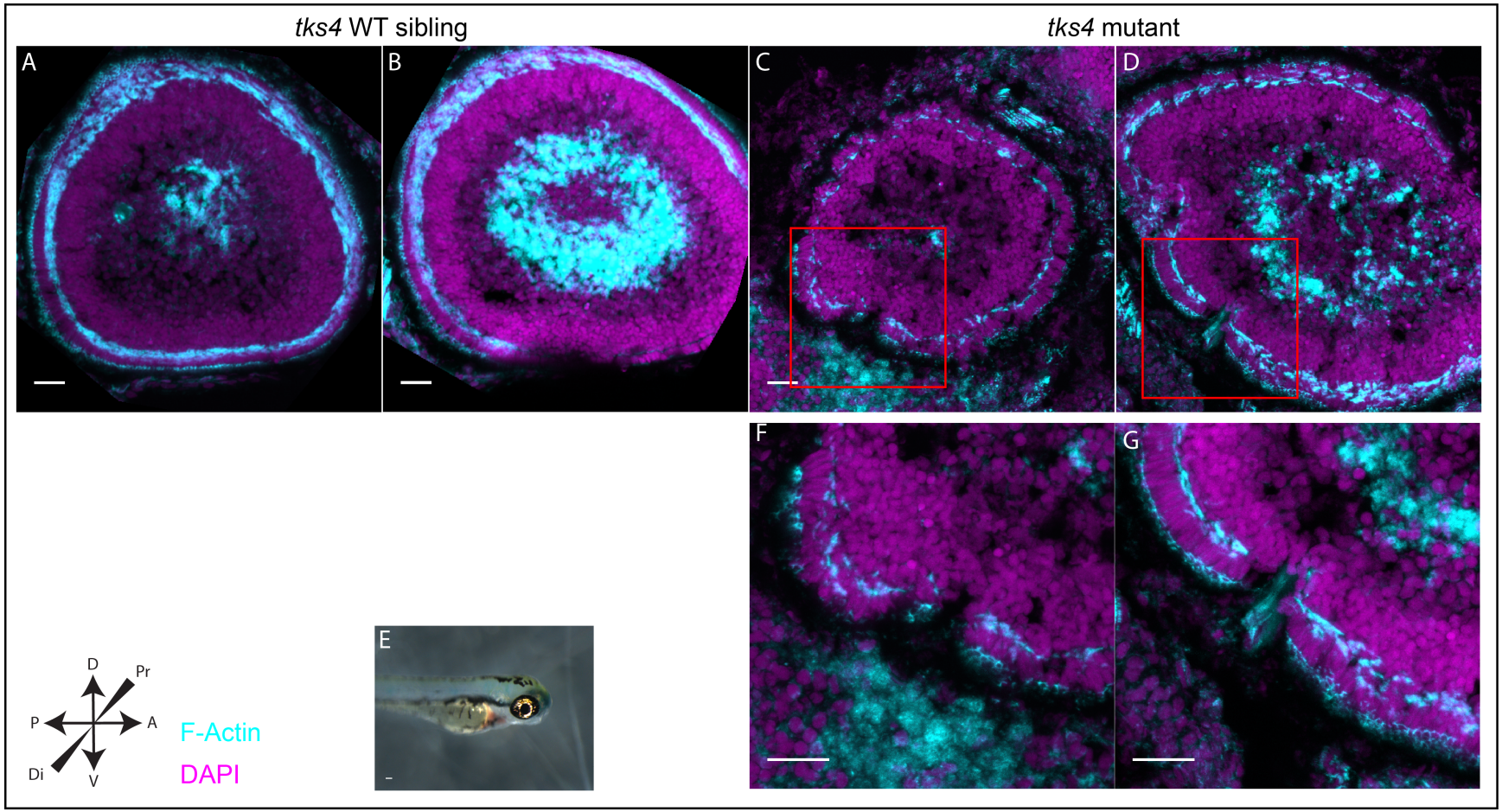

Figure 3: *tks4* mutants have mild coloboma

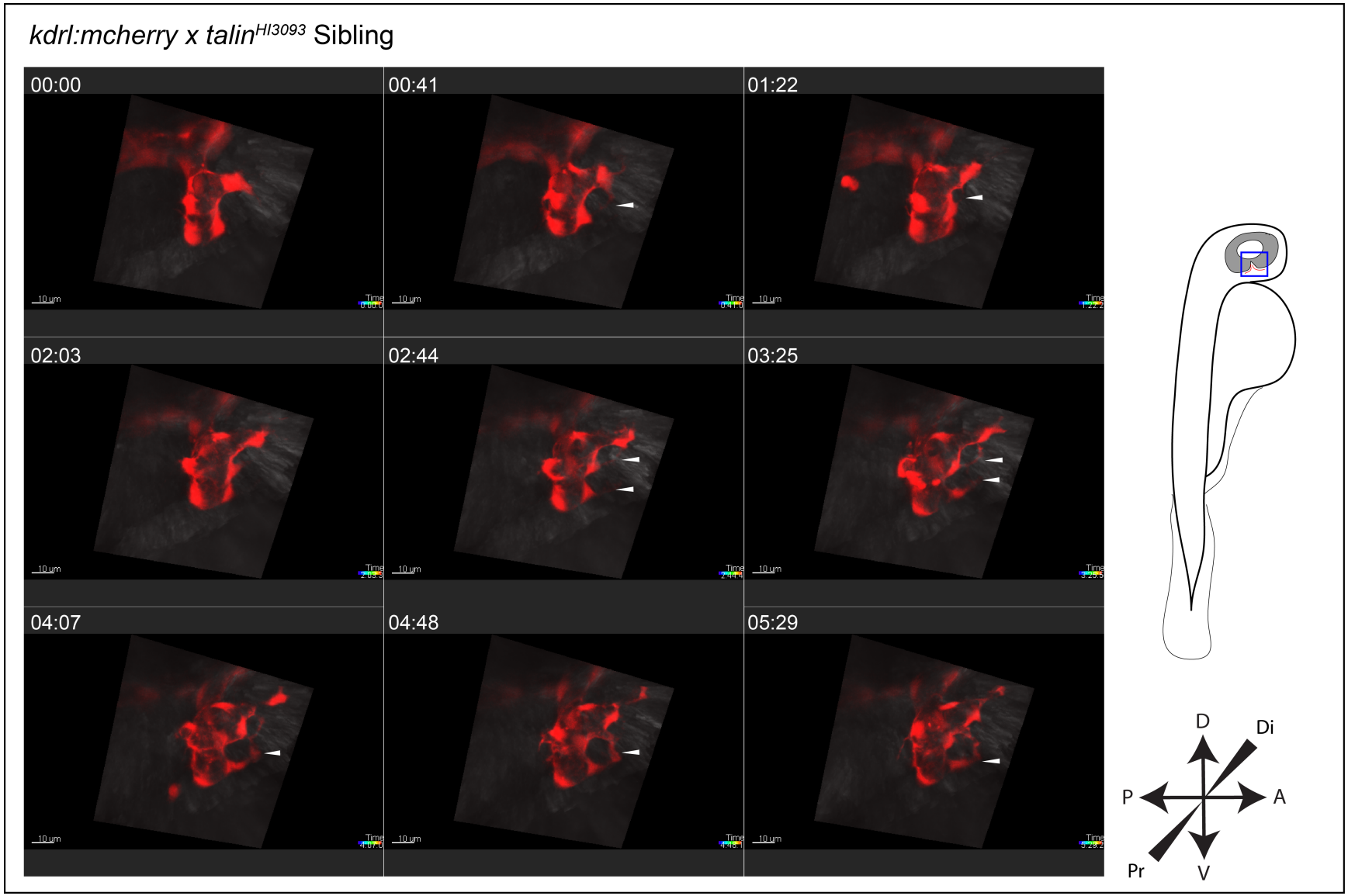

Figure 4: Live imaging of wildtype hyaloid vasculature show vascular extensions on ventral surface of optic cup

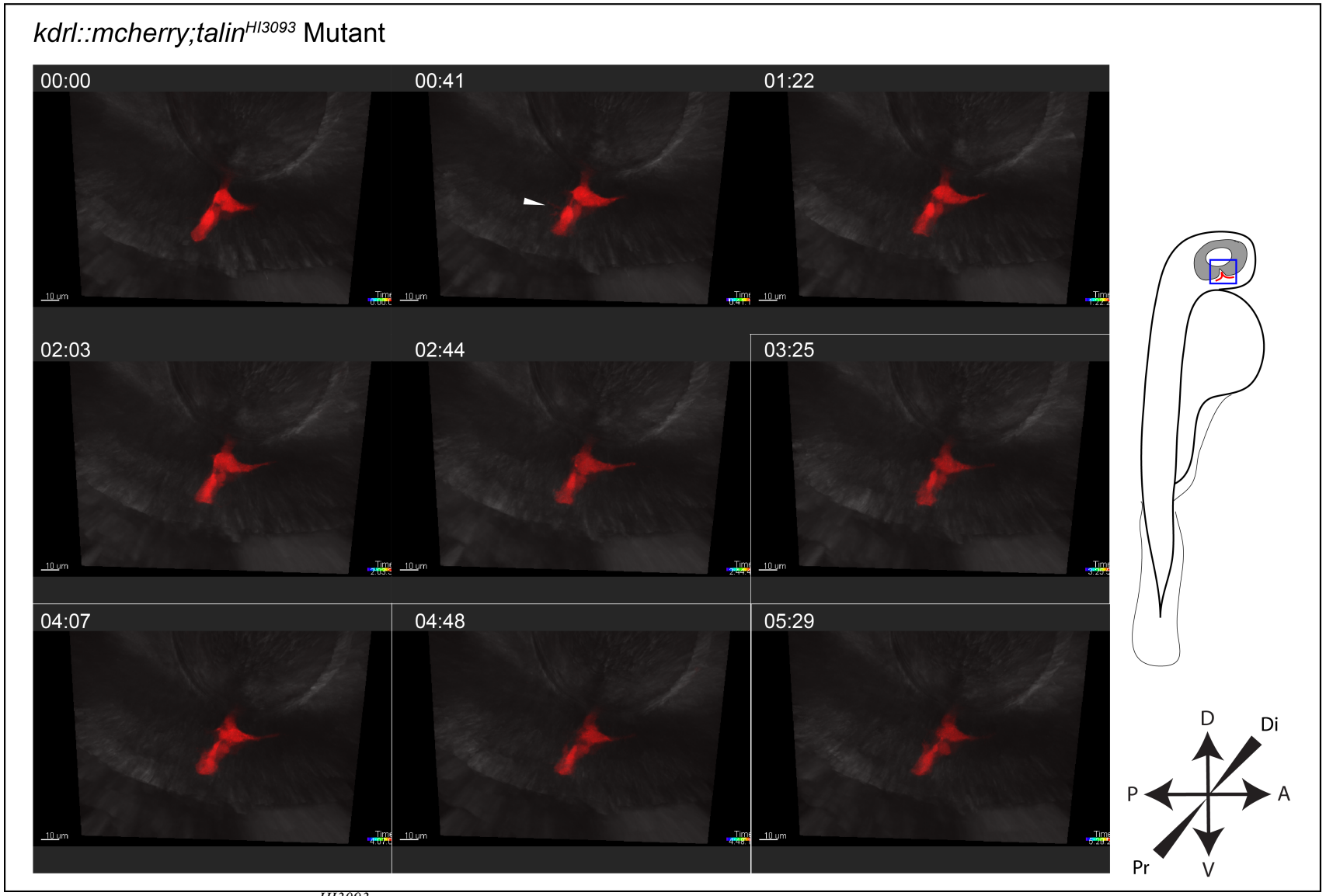

Figure 5: Live imaging of *talin*^{HI3093} mutant hyaloid vasculature shows collapsed lumen and no vascular extension

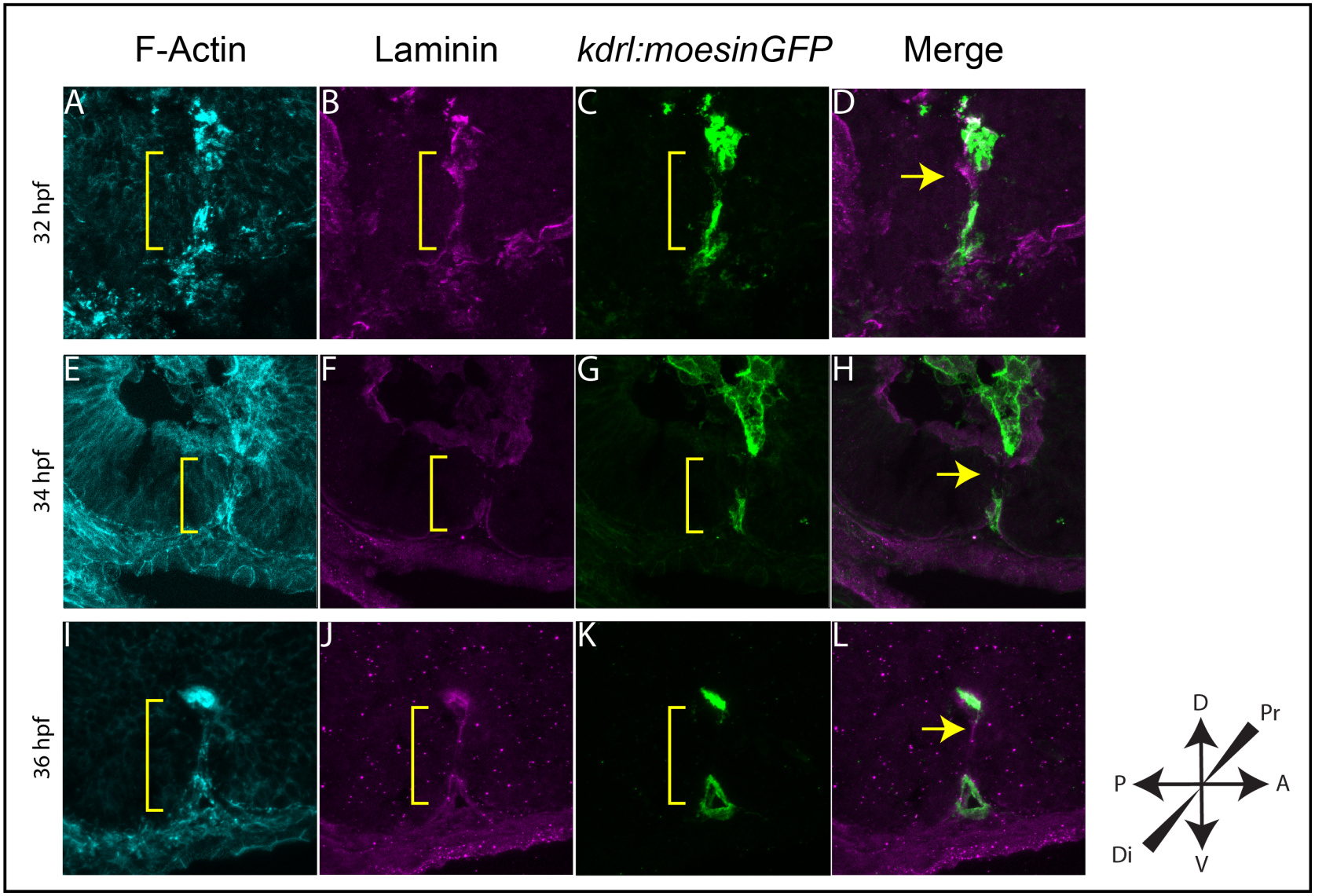

Figure 6: Hyaloid vasculature cells are not present in choroid fissure during basement membrane breakdown

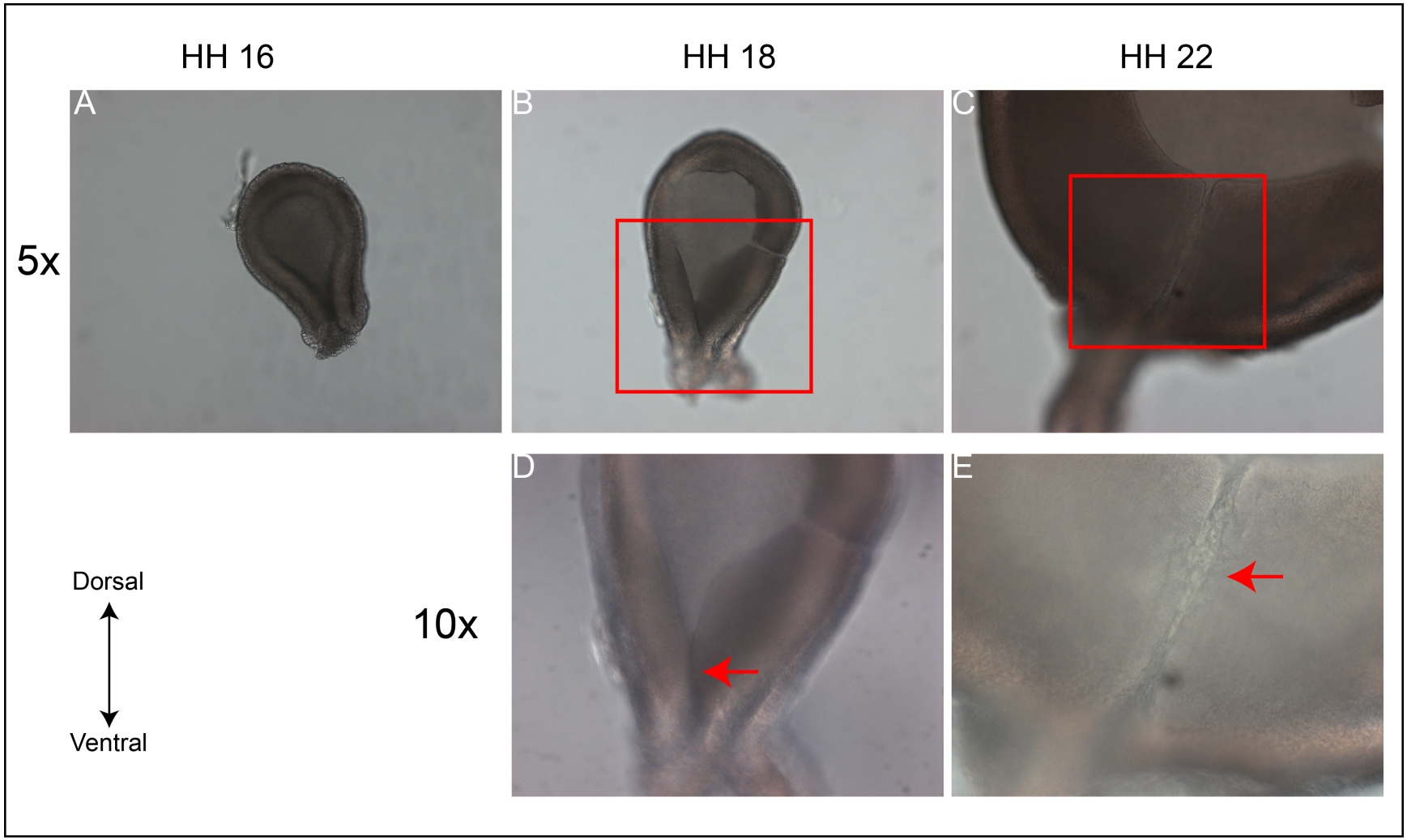

Figure 7: Mesenchymal cells invade chicken choroid fissure during timeframe of closure

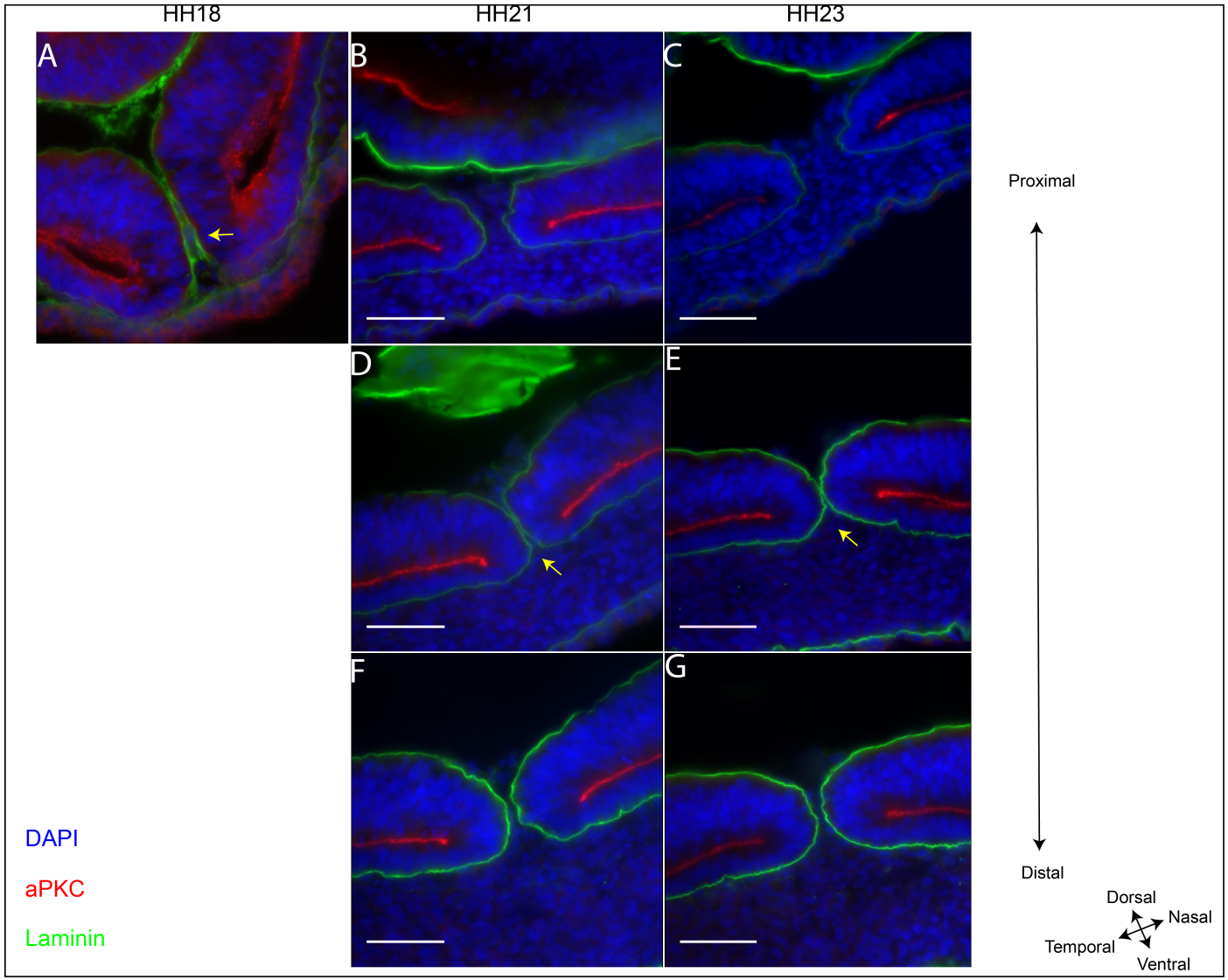

Figure 8: Immunohistochemistry of chicken choroid fissure shows no breakdown of ECM during invasion of mesenchymal cell

ECM breakdown is normal in *talin*^{HI3093Tg} mutants

Podosomes degrade ECM through the accumulation of high concentrations of actin that facilitate protrusions into the extracellular space[17,48,49]. Talin is a linker protein that helps attach the actin cytoskeleton to the cell membrane, and also links extracellular proteins such as Integrin to Actin[32,36,50]. Talin is a part of the actin cytoskeleton needed for functional podosome mediated degradation [37]. Our working hypothesis states that Talin is required for CFC through generating podosomes within the CF. To test this hypothesis, we utilized the *talin*^{HI3093Tg} mutant line to study the requirement for talin during CFC. There are two phenotypic classes of *talin*^{HI3093Tg} mutants: both have cardiac edema, but ocularly, there are those with mild coloboma, and those with severe coloboma. In this thesis, I explored the mild class of mutants who present with coloboma at the distal region of the eye.

To determine whether Talin is required to degrade the ECM, I sectioned fixed *talin*^{HI3093Tg} sibling and mutant embryos collected at both 2dpf and 3dpf. During the second phase of CFC, the ECM on the edges of the CF begins to breakdown. Laminin-111 is an ECM component that can be used to determine if basement membrane breakdown has occurred. Both *talin*^{HI3093Tg} siblings and mutants showed a lack of laminin staining in the choroid fissure by 3pf (Figure 1C, D), suggesting that Talin does not play a role in basement membrane breakdown during CFC. To determine if the coloboma present in the mild mutants is due to a delay, I examined *talin*^{HI3093Tg} sibling and mutant embryos at 2 dpf. No laminin was detected within the choroid fissure of mutant embryos, suggesting that there is no delay in ECM breakdown (figure 1A, B). This suggests that even though Talin is found within podosomes, it may not be required

to facilitate ECM breakdown, and other podosome components should be investigated to determine whether podosomes are required for CFC.

Mutation of tks4 results in mild coloboma

The podosome component protein tks4 is responsible for recruitment of molecules, such as MMPs, with enzymatic activity that are capable of degrading ECM components[17,26]. Though podosomes have not been shown to function during CFC previously, mRNA for podosome components *tks4, mmp2* and *mmp14a* is expressed in the choroid fissure at 40hpf (Unpublished data, Lee& Gross). Experiments in cell culture show that Tks4 is required for podosome-mediated degradation of the ECM to occur [25]. To determine if podosomes are responsible for ECM breakdown during CFC, we disrupted Tks4 expression, hypothesizing that mutation of *tsk4* would result in coloboma. Disruption was achieved using transcription activator-like effector nucleases (TALENs) targeted to the *tks4* locus in the first exon (Figure 2A). Nucleases on the end of the TALEN constructs create a double stranded break between the two recognition sites[30,51] that is repaired by error-prone non-homologous end joining, which can result in insertions or deletions. The sperm of F0 adults was genotyped to determine carriers of deleterious mutations in the *tks4* locus. A founder parent containing an 11 base pair insertion following the start codon (Figure 2B, red) was discovered, This insertion is predicted to result in a frameshift, and causes a nonsense mutation that truncates the tks4 protein after the 15th amino acid (Figure 2C, asterisks). *tks4* heterozygous adults were incrossed resulting in *tks4*$^{-/-}$ embryos (Figure 2E); these were phenotypically indistinguishable from their siblings (Figure 2D). None of the mutants displayed an obvious coloboma.

To assess whether CFC is at all disrupted in *tks4* mutants, I sectioned embryos and performed immunohistochemical analysis using F-actin and DAPI to visualize retinal structure at 3dpf, when CFC is complete. F-actin is concentrated within the plexiform layers of the zebrafish retina at 3dpf, with no ventral accumulation present in what was once the choroid fissure (Figure 3A). In the *tks4*$^{-/-}$ mutant, there is a gap in the temporal side of the ventral retina, with a concentration of F-actin extending into the retina (Figure 3 B, C). Because this gap is on the ventral surface of the retina, it is possible that this is a part of the choroid fissure that has not fused during development. This preliminary result suggests that *tks4* mutants may possess a mild coloboma. Though this result is not definitive in demonstrating a required role for *tks4* in CFC, it does suggest that podosomes may function during ECM degradation in CFC.

Actin within hyaloid vasculature does not localize to areas of ECM breakdown during CFC

My central hypothesis is that ECM breakdown during CFC is mediated by podosomes present in hyaloid vasculature cells migrating through the choroid fissure. In addition to coloboma, *talin*^{HI3093Tg} mutants have abnormal hyaloid vasculature (Chanjae Lee, unpublished results. To determine whether the podosomes are present within the hyaloid vasculature during CFC, I chose to investigate cell dynamics in the hyaloid vasculature during CFC, using live imaging of *talin*^{HI3093Tg} Tg(*kdrl:mCherry)* lines. The *kdrl:mCherry* transgene is expressed within the hyaloid vasculature, localized to the cell membranes, and was used to observe whether extensions emanate from hyaloids cells within the CF. *kdrl:mCherry;talin*^{HI3093Tg} siblings that did not carry the *talin*^{HI3093Tg} mutation showed normal lumen morphology within the hyaloid vasculature (Figure 4). The *kdrl:mCherry;talinHI3093Tg* mutants showed a collapsed lumen, showing that there is a defect within the hyaloid vasculature during CFC (Figure 5). Live

imaging also allowed us to capture images of extensions emanating from the hyaloid vasculature in *kdrl:mCherry;talin*^{HI3093Tg} siblings. Extensions from the hyaloid vasculature were hypothesized to be podosomes in previous work from the lab (Chanjae Lee, unpublished results). However, 3-D projection of these extensions from the hyaloid vasculature shows that they project along the ventral surface of the optic cup (Figure 4, arrowheads). The extensions from the hyaloid vasculature also make contact and fuse with one another, suggesting that they are not podosomes, and instead may be part of another unrelated process within the vasculature. In the *kdrl:mCherry;talin*^{HI3093Tg} mutants, the cells extend fewer projections from the vasculature, and these projections fail to make contact with one another (Figure 5, arrowheads).

Though we showed that previously characterized extensions coming from the hyaloid vasculature are not characteristic of podosomes (unpublished data), we had not determined whether the vasculature is capable of degrading the ECM. To determine whether actin-based protrusions from the hyaloid vasculature participate in degradation of ECM during CFC, I investigated the initial stages of ECM breakdown. Tg(*kdrl:moesinGFP*) embryos were collected at 32, 34, and 36 hpf and sectioned in the sagittal plane of the organism. I performed immunohistochemical analyses to visualize basement membrane (laminin-111), vascular cell actin (*kdr1:moesinGFP*), and F-actin throughout the CF (phalloidin). ECM breakdown during CFC initiates between 31 and 36 hpf (unpublished data). At 32hpf, the laminin surrounding the leading edges of the choroid fissure is intact, consistent with previous analysis (Figure 6B). Actin within the hyaloid vasculature is present in all but the central most region of the choroid fissure (Figure 6C). F-actin has an increased accumulation within the CF, suggesting more activity in this site (Figure 6A). Merging the images from the laminin and Tg(*kdrl:moesinGFP*) show that there are CF regions with intact basement membrane that lack hyaloid vasculature (Figure 6D).

This is even more apparent as CFC progresses. At 34hpf, the ECM between the two edges of the retina is degraded in the central portion of the choroid fissure (Figure 6F). Actin within the hyaloid vasculature does not colocalize with laminin along the leading edges of the retina, suggesting no interaction between actin within the hyaloid vasculature and ECM breakdown at 34hpf (Figure 6E, G). This is again observed in 36hpf Tg(*kdrl:moesinGFP*) embryos, where hyaloid actin is not present despite persistence of laminin in the CF (Figure 6J-L). There is F-actin present within this area, suggesting that actin plays a role in ECM breakdown (Figure 6I, arrowhead). However, these data do not support a role for the hyaloid vasculature in degrading the ECM during CFC. It is still possible that the hyaloid vasculature participates in ECM breakdown, however more concrete evidence is needed to determine what cell type is responsible for ECM breakdown. Direct localization of podosome components within the CF may determine whether podosomes are responsible for ECM breakdown, and if podosomes are present, which cell type is responsible for ECM breakdown during CFC.

Investigation of CFC in chick is complicated by an avian ocular structure, the pecten

To use chicken (*G. gallus*) as a new model organism for studying CFC, I first needed to determine when CFC occurs. To determine the timing of CFC in chicken, I took whole mount images of dissected chicken retinas. Chicken embryos were staged according to Hamburger and Hamilton staging [47]. At HH16, the two edges of the retina approach each other, but are not fused (Figure 7A). This can be determined mechanically by passing a small wire through the edges of the fissure. The HH16 retina allows the wire to pass smoothly, suggesting the retina was not tightly apposed at this stage of development (data now shown). HH18 embryos show tight apposition of the two edges of the retina, forming a seam through which a wire cannot pass

(Figure 7B). Higher magnification shows tight apposition of the two edges of the retina, suggesting that this is the point at which choroid closure begins to occur (Figure 7D, red arrow). However, at HH22, the retina has a gap that emerges between the two edges of the retina (Figure 7C). Higher magnification reveals a population of mesenchymal cells within the fissure that separate the two edges of the retina. This is interesting, as the invasion of the hyaloid vasculature in zebrafish begins at 19hpf, long before the two edges of the retina meet[39]. This led me to investigate whether basement membrane is broken down during the time that the two edges of the retina become apposed to one another. At HH18, the apposed edges of the retina are surrounded by laminin, meaning ECM breakdown has not occurred (Figure 8A). There is a single mesenchymal cell that is seen residing within the fissure (Figure 8A, yellow arrowhead). At HH21 (E3.5), the retina remains tightly apposed in the central section of the fissure, but invasion of mesenchymal cells is observed both at the proximal and distal edges (Figure 8B,D,F). This is also the case with HH23 embryos (E4.0) The space between the choroid fissure is much wider, and more mesenchymal cells are present (Figure 8C,E,G). In the medial portion of the fissure, the two sides of the retina remain apposed (Figure 8E). These findings suggest that CFC in chicken is prevented as mesenchymal cells pass through to create the pecten, as the gap between the cells does not seem to close. However, chick eye development differs from that of humans and fish due to a structure within the eye called the pecten[52]. Made up of mesenchymal cells, the pecten is a housing for the hyaloid vasculature, and both tissues remain within the eye into adulthood. Though the CFC in chicken seems to be different from that of humans or zebrafish, it is likely that some mechanisms are preserved. Further investigation of the processes in chicken may help us understand what aspects are conserved between chick and other model organisms, and what has diverged over time.

Discussion

In this thesis, I have shown that while there is support for the hypothesis that podosomes are responsible for degrading the ECM during CFC, more research needs to be done to determine which molecular components are critical for facilitating this process. We first sought to determine how Talin affects ECM breakdown during CFC. The talin^{HI3093Tg} mutant line possesses both a mind and a severe phenotype. I studied the mild mutant, which presents with coloboma only at the distal portion of the retina. Though Talin is a part of podosome machinery[37], and *talin*^{HI3093Tg} mutants possess colobomas (Chanjae Lee, unpublished results), I found that these do not correlate with defects in ECM breakdown, suggesting Talin does not participate in ECM breakdown during CFC in mild mutants. At 2 dpf, mild *talin*^{HI3093Tg} mutant siblings lack laminin along the former choroid fissure (Figure 1A). This is similar to what is seen in sibling embryos of the same age (Figure 1B). The absence of laminin within the choroid fissure of the *talin*^{HI3093Tg} mutants suggests, based on data presented here, that Talin is not required for ECM breakdown. However, previous data does show that laminin remains within the choroid fissure in severe *talin*^{HI3093Tg} mutants (Chanjae Lee, Unpublished results). The difference in phenotype between the mild and severe *talin*^{HI3093Tg} mutants could be due to the difference in Talin deposited in individual eggs[53]. When this maternal contribution of Talin is depleted could determine the severity of the mutants seen in this study. In addition, actin-binding proteins are also required for the third phase of CFC, fusion between the two edges of the optic cup[54]. More investigation of the role of Talin

both the mild and severe mutants will aid in understanding the specific role of Talin in CFC.

After determining that Talin may not be required in ECM breakdown during CFC, a mutant *tks4* line was created using TALENs by a previous member of the lab (Jiwoon Lee, unpublished results) to determine if mutation of core podosome component genes affect CFC. The *tks4* phenotype is subtle, as mutants are indistinguishable from WT by visual observation. Once sectioned, there is a mild coloboma that can be seen in *tks4*$^{-/-}$ mutants (Figure 3C, D). Though this datum is not conclusive in determining the specific role of *tks4* in CFC, it does show that it could be required for proper fissure closure. There are a number of reasons why the phenotype may not be as severe as one would expect from a knockout of a major podosome component. First, Tks4 is downstream of Tks5, and as such, Tks5 may be able to compensate for the loss of Tks4[17]. Second, if there is a maternal contribution of Tks4, it may be necessary to deplete the maternal contribution to fully determine the effect that mutating *tks4* has on CFC. To achieve a tks4 null background, an incross of F2 heterozygous parents fish would be performed, and tks4$^{-/-}$ mutants would be grown to adulthood before mating. Another technique to deplete maternal contribution of Tks4 in embryos would be to use morpholino oligos (MO). MOs are able to bind to single stranded mRNA and prevent proper splicing or translation[55]. Previous work using MO has shown that Tks5 is needed for proper neural crest migration, but the morphant embryos were not scored for coloboma[23]. Though MO are an incredibly powerful too to utilize, they also must be compared to mutants to verify that the phenotype presented is due to the MO and not to off target effects[56]. Using this

knowledge, a future experiment to consider will be to mutate *tks5* via a targeted mutagenic method[57] and determine if there is a phenotype present, as a mutation in *tks5* should halt podosome formation. A combination of mutations in both *tks4* and *tks5* could result in a complete coloboma if podosomes are involved in CFC. Furthermore, as MMPs are the enzymes responsible for breaking down the ECM in podosomes, targeted mutagenesis could be another way to determine if this group of genes is required for ECM breakdown in CFC. MMPs that have been shown to be important for ECM breakdown by podosomes include *mmp2, mmp9, and mmp14a*[17,27,29]. Determining the effect that other podosome components have on CFC could further determine if podosomes are required for ECM breakdown.

Previous data suggested that the hyaloid vasculature was affected by the *talin*^{HI3093Tg} mutation. I imaged Tg(*kdrl:mCherry*);*talin*^{HI3093Tg} embryos using a confocal microscope between 42 - 48 hpf to observe the morphology of the hyaloid vasculature. In normal development, the hyaloid vasculature fills the lumen between the two edges of the choroid fissure, supplying nutrients to the developing lens (Figure 4). The hyaloid vasculature in *talin*^{HI3093Tg} mutants is collapsed within the choroid fissure (Figure 5). The cells within the hyaloid vasculature do not travel towards the lens, remaining stationary until the two edges of the CF are brought together. In addition, the *talin*^{HI3093Tg} siblings have hyaloid vasculature that sends projections along the ventral surface of the choroid fissure. These projections are observed in *talin*^{HI3093Tg} mutants, but they are less pronounced and do not make connection with other projections (Figure 5, arrowhead). This suggests Talin is required for cell movement within the hyaloid vasculature. The

decrease in the number of projections seen within the hyaloid vasculature suggests that Talin is also involved creating these projections. These projections were initially thought to be evidence of podosomes within the hyaloid vasculature, but the data presented in this thesis do not support that hypothesis.

Data presented within this study suggest that the hyaloid vasculature does not localize with ECM breakdown within the CF. This suggests that the hyaloid vasculature does not play a role in CFC. Laminin is present within the ECM the choroid fissure, and we utilized this protein to determine presence of the ECM during CFC. Merged images of immunohistochemical staining show laminin expression is present in the region of the choroid fissure where the hyaloid vasculature was absent (Figure 6D, H, L). This suggests that the hyaloid vasculature is not actively participating in the ECM breakdown seen in CFC. It is possible that as the vasculature travels through the choroid fissure, it deposits signals that induce podosome formation, such as VEGF and TGF[58–60]. To exclude the hyaloid vasculature's involvement in CFC completely, a mutant that lacks vasculature would be required. The *cloche* mutant fails to develop head vasculature, and as such, does not develop hyaloid vasculature[61–63]. Observing whether or not CFC is affected in *cloche* mutants can determine the requirement of the hyaloid vasculature in degrading the ECM. Though the hyaloid vasculature does not seem to be involved, other cells within the CF may possess podosomes to degrade ECM. Two other cell types that are involved in CFC are the retina and the RPE. Though retinal progenitor cells (RPC) have not been shown to possess podosomes, microglial cells and other neuronal cells have been shown to use podosomes in growth cones for moving through the body [19,24].

CFC in other model organisms, such as mouse, shows that there are cellular protrusions emanating from the retina and crossing the choroid fissure, which could be another avenue to explore in future experiments[9–11]. These options may add a new layer of complexity to the current model of CFC, and shed light as to the exact mechanism underlying ECM breakdown.

Data presented in this study suggest that CFC in chicken does not happen similar to zebrafish and human models. Though the two edges of the CF approach each other and make contact at HH18, by HH21 there are mesenchymal cells that invade the choroid fissure (Figure 8 A, B, C). At HH23, the two edges of the retina remain open, with the hyaloid vasculature and periocular mesenchyme remaining within the choroid fissure (Figure 8C). When the two edges of the retina are apposed at HH18 (Figure 8A), cells are present within the CF (Figure 8A, arrowhead). The CF is separated, and the precursory pecten pushes the two edges of the retina apart. The central parts of the CF remain apposed, but laminin is not degraded as eye development progresses (Figure 8D, E). This means that CFC closure does not occur in the same manner as in zebrafish and humans. Neither species has a pecten, nor hyaloid vasculature that persists into adulthood[52]. However, other mechanisms are similar such as the formation of the optic cup and the molecular signals that we may still gain from studying the chick. Periocular mesenchyme cells are thought to be required for proper CFC, and are important for signaling proper morphogenesis of the eye [64]. As such, chicken has potential to be used in developmental processes that lead up to CFC. Chicken eyes can also be subjected to electroporation, allowing us to see what effects introducing a large amount of a DN or

CA construct would have on eye development[44,43]. A complete time course of the approach of the leading edges of the retina needs to be completed, where the dynamics of the apposition and invasion of the pecten and hyaloid vasculature can be visualized to determine if there is a place along the choroid fissure in which fusion does occur.

Our hypothesis that the hyaloid vasculature degrades the ECM in zebrafish CFC was not supported in this thesis. However, data presented in this thesis suggest that more work needs to be done to understand what role podosomes have in facilitating ECM breakdown. Combining data gathered from various model organisms will help determine what are the molecular underpinnings of ECM breakdown during CFC.

References

1. Schmitt, E. A. & Dowling, J. E. Early-eye morphogenesis in the zebrafish, Brachydanio rerio. *J. Comp. Neurol.* **344,** 532–542 (1994).

2. Pagon, R. Ocular coloboma. *Surv. Ophthalmol.* **45,** 223–236 (1981).

3. Chang, L., Blain, D., Bertuzzi, S. & Brooks, B. P. Uveal coloboma: clinical and basic science update. *Curr. Opin. Ophthalmol.* **17,** 447–70 (2006).

4. Gregory-Evans, C. Y., Williams, M. J., Halford, S. & Gregory-Evans, K. Ocular coloboma: a reassessment in the age of molecular neuroscience. *J. Med. Genet.* **41,** 881–891 (2004).

5. Brodsky, M. C. Congenital anomalies of the optic disc. *Walsh Hoyt's Clin. neuro-ophthalmology* **29,** 151–195 (2005).

6. Uhumwangho, O. M. & Jalali, S. Chorioretinal coloboma in a paediatric population. *Eye (Lond).* **28,** 728–33 (2014).

7. FitzPatrick, D. R. & Van Heyningen, V. Developmental eye disorders. *Curr. Opin. Genet. Dev.* **15,** 348–353 (2005).

8. Bibliowicz, J., Tittle, R. K. & Gross, J. M. *Toward a better understanding of human eye disease insights from the zebrafish, Danio rerio. Progress in molecular biology and translational science* **100,** (Elsevier Inc., 2011).

9. Hero, I. The optic fissure in the normal and microphthalmic mouse. *Exp. Eye Res.* **49,** 229–239 (1989).

10. Hero, I. Optic fissure closure in the normal cinnamon mouse: An ultrastructural study. *Investig. Ophthalmol. Vis. Sci.* **31,** 197–216 (1990).

11. Hero, I., Farjah, M. & Scholtz, C. L. The prenatal development of the optic fissure in colobomatous microphthalmia. *Investig. Ophthalmol. Vis. Sci.* **32,** 2622–2635 (1991).

12. Tsuji, N., Kita, K., Ozaki, K., Narama, I. & Matsuura, T. Organogenesis of mild ocular coloboma in FLS mice: failure of basement membrane disintegration at optic fissure margins. *Exp. Eye Res.* **94,** 174–8 (2012).

13. Sehgal, R., Karcavich, R., Carlson, S. & Belecky-Adams, T. L. Ectopic Pax2 expression in chick ventral optic cup phenocopies loss of Pax2 expression. *Dev. Biol.* **319,** 23–33 (2008).

14. Torres, M., Gómez-Pardo, E. & Gruss, P. Pax2 contributes to inner ear patterning and optic nerve trajectory. *Development* **122,** 3381–3391 (1996).

15. Sanyanusin, P. *et al.* Mutation of the PAX2 gene in a family with optic nerve colobomas, renal anomalies and vesicoureteral reflux. *Nat. Genet.* **9,** 358–364 (1995).

16. Linder, S. The matrix corroded: podosomes and invadopodia in extracellular matrix degradation. *Trends Cell Biol.* **17,** 107–117 (2007).

17. Murphy, D. a & Courtneidge, S. a. The 'ins' and 'outs' of podosomes and invadopodia: characteristics, formation and function. *Nat. Rev. Mol. Cell Biol.* **12,** 413–26 (2011).

18. Cawston, T. E. & Young, D. a. Proteinases involved in matrix turnover during cartilage and bone breakdown. *Cell Tissue Res.* **339,** 221–235 (2010).

19. Vincent, C., Siddiqui, T. a & Schlichter, L. C. Podosomes in migrating microglia: components and matrix degradation. *J. Neuroinflammation* **9,** 190 (2012).

20. Blouw, B., Seals, D. F., Pass, I., Diaz, B. & Courtneidge, S. a. A role for the podosome/invadopodia scaffold protein Tks5 in tumor growth in vivo. *Eur. J. Cell Biol.* **87,** 555–567 (2008).

21. Hagedorn, E. J. *et al.* Integrin Acts Upstream of Netrin Signaling to Regulate Formation of the Anchor Cell's Invasive Membrane in C. elegans. *Dev. Cell* **17,** 187–198 (2009).

22. Hagedorn, E. J. *et al.* ADF/cofilin promotes invadopodial membrane recycling during cell invasion in vivo. *J. Cell Biol.* **204,** 1209–18 (2014).

23. Murphy, D. a. *et al.* A Src-Tks5 pathway is required for neural crest cell migration during embryonic development. *PLoS One* **6,** (2011).

24. Santiago-Medina, M., Gregus, K. a., Nichol, R. H., O'Toole, S. M. & Gomez, T. M. Regulation of ECM degradation and axon guidance by growth cone invadosomes. *Development* **142,** 486–496 (2015).

25. Buschman, M. D. *et al*. The Novel Adaptor Protein Tks4 (SH3PXD2B) Is Required for Functional Podosome Formation. **20,** 1302–1311 (2009).

26. Courtneidge, S. A. Cell migration and invasion in human disease: the Tks adaptor proteins. *Biochem. Soc. Trans.* **40,** 129–132 (2012).

27. Frittoli, E., Palamidessi, A., Disanza, A. & Scita, G. Secretory and endo/exocytic trafficking in invadopodia formation: The MT1-MMP paradigm. *Eur. J. Cell Biol.* **90,** 108–114 (2011).

28. Gawden-Bone, C. *et al*. Dendritic cell podosomes are protrusive and invade the extracellular matrix using metalloproteinase MMP-14. *J. Cell Sci.* **123,** 1427–1437 (2010).

29. Xiao, H. *et al*. The protein kinase C cascade regulates recruitment of matrix metalloprotease 9 to podosomes and its release and activation. *Mol. Cell. Biol.* **30,** 5545–5561 (2010).

30. Huang, P. *et al*. Heritable gene targeting in zebrafish using customized TALENs. *Nat. Biotechnol.* **29,** 699–700 (2011).

31. Hwang, W. Y., Peterson, R. T. & Yeh, J.-R. J. Methods for targeted mutagenesis in zebrafish using TALENs. *Methods* **69,** 76–84 (2014).

32. Bouaouina, M., Lad, Y. & Calderwood, D. a. The N-terminal domains of talin cooperate with the phosphotyrosine binding-like domain to activate β1 and β3 integrins. *J. Biol. Chem.* **283,** 6118–6125 (2008).

33. Spinardi, L. & Marchisio, P. C. Podosomes as smart regulators of cellular adhesion. *Eur. J. Cell Biol.* **85,** 191–194 (2006).

34. Schachtner, H., Calaminus, S. D. J., Thomas, S. G. & Machesky, L. M. Podosomes in adhesion, migration, mechanosensing and matrix remodeling. *Cytoskeleton* **70,** 572–589 (2013).

35. Janoštiak, R., Pataki, A. C., Brábek, J. & Rösel, D. Mechanosensors in integrin signaling: The emerging role of p130Cas. *Eur. J. Cell Biol.* **93,** 445–454 (2014).

36. Roca-Cusachs, P., Gauthier, N. C., Del Rio, A. & Sheetz, M. P. Clustering of alpha(5)beta(1) integrins determines adhesion strength whereas alpha(v)beta(3) and talin enable mechanotransduction. *Proc. Natl. Acad. Sci. U. S. A.* **106,** 16245–16250 (2009).

37. Beaty, B. T. *et al*. Talin regulates moesin-NHE-1 recruitment to invadopodia and promotes mammary tumor metastasis. *J. Cell Biol*. **205,** 737–751 (2014).

38. Saint-Geniez, M. & D'Amore, P. a. Development and pathology of the hyaloid, choroidal and retinal vasculature. *Int. J. Dev. Biol*. **48,** 1045–1058 (2004).

39. Hartsock, A., Lee, C., Arnold, V. & Gross, J. M. In vivo analysis of hyaloid vasculature morphogenesis in zebrafish: A role for the lens in maturation and maintenance of the hyaloid. *Dev. Biol*. **394,** 327–39 (2014).

40. Stupack, D. G. & Cheresh, D. a. ECM remodeling regulates angiogenesis: endothelial integrins look for new ligands. *Sci. STKE* **2002,** pe7 (2002).

41. Seano, G., Daubon, T., Génot, E. & Primo, L. Podosomes as novel players in endothelial biology. *Eur. J. Cell Biol*. **93,** 405–412 (2014).

42. Seano, G. & Primo, L. Podosomes and invadopodia: tools to breach vascular basement membrane. *Cell Cycle* **14,** 1370–1374 (2015).

43. Momose, T. *et al*. Efficient targeting of gene expression in chick embryos by microelectroporation. *Dev. Growth Differ*. **41,** 335–344 (1999).

44. Yasuda, K., Momose, T. & Takahashi, Y. Applications of microelectroporation for studies of chick embryogenesis. *Dev. Growth Differ*. **42,** 203–206 (2000).

45. Cermak, T. *et al*. Erratum: Efficient design and assembly of custom TALEN and other TAL effector-based constructs for DNA targeting (Nucleic Acids Research (2011) 39 (e82) DOI: 10.1093/nar/gkr218). *Nucleic Acids Res*. **39,** 7879 (2011).

46. Wang, Y. *et al*. Moesin1 and Ve-cadherin are required in endothelial cells during in vivo tubulogenesis. *Development* **137,** 3119–3128 (2010).

47. Hamburger, V. & Hamilton, H. A Series of Normal Stages in the Development of the Chick Embryo. *Dev. Dyn*. **88,** 231–272 (1992).

48. Linder, S. & Aepfelbacher, M. Podosomes: Adhesion hot-spots of invasive cells. *Trends Cell Biol*. **13,** 376–385 (2003).

49. Linder, S., Wiesner, C. & Himmel, M. Degrading Devices: Invadosomes in Proteolytic Cell Invasion. *Annu. Rev. Cell Dev. Biol*. **27,** 185–211 (2011).

50. Rossier, O. *et al*. Integrins β1 and β3 exhibit distinct dynamic nanoscale organizations inside focal adhesions. *Nat. Cell Biol*. **14,** 1057–1067 (2012).

51. Miller, J. C. *et al*. A TALE nuclease architecture for efficient genome editing. *Nat. Biotechnol*. **29,** 143–148 (2011).

52. Wolburg, H., Liebner, S., Reichenbach, A. & Gerhardt, H. The Pecten Oculi of the Chicken: A Model System for Vascular Differentiation and Barrier Maturation. *Int. Rev. Cytol*. **187,** 111–159 (1999).

53. Ryu, S., Holzschuh, J., Erhardt, S., Ettl, A.-K. & Driever, W. Depletion of minichromosome maintenance protein 5 in the zebrafish retina causes cell-cycle defect and apoptosis. *Proc. Natl. Acad. Sci. U. S. A*. **102,** 18467–18472 (2005).

54. Kurita, R., Tabata, Y., Sagara, H., Arai, K. I. & Watanabe, S. A novel smoothelin-like, actin-binding protein required for choroidal fissure closure in zebrafish. *Biochem. Biophys. Res. Commun*. **313,** 1092–1100 (2004).

55. Nasevicius, a & Ekker, S. C. Effective targeted gene 'knockdown' in zebrafish. *Nat. Genet*. **26,** 216–220 (2000).

56. Kok, F. O. *et al*. Reverse Genetic Screening Reveals Poor Correlation between Morpholino-Induced and Mutant Phenotypes in Zebrafish. 97–108 (2015).

57. Hisano, Y., Ota, S. & Kawahara, A. Genome editing using artificial site-specific nucleases in zebrafish. *Dev. Growth Differ*. **56,** 26–33 (2014).

58. Wang, J. *et al*. GIT1 mediates vegf-induced podosome formation in endothelial cells. Critical role for PLC?? *Arterioscler. Thromb. Vasc. Biol*. **29,** 202–208 (2009).

59. Weis, S., Cui, J., Barnes, L. & Cheresh, D. Endothelial barrier disruption by VEGF-mediated Src activity potentiates tumor cell extravasation and metastasis. *J. Cell Biol*. **167,** 223–229 (2004).

60. Varon, C. *et al*. Transforming Growth Factor β Induces Rosettes of Podosomes in Primary Aortic Endothelial Cells. *Mol. Cell. Biochem*. **26,** 3582–3594 (2006).

61. Stainier, D. Y., Weinstein, B. M., Detrich, H. W., Zon, L. I. & Fishman, M. C. Cloche, an early acting zebrafish gene, is required by both the endothelial and hematopoietic lineages. *Development* **121,** 3141–3150 (1995).

62. Liao, W. *et al*. The zebrafish gene cloche acts upstream of a flk-1 homologue to regulate endothelial cell differentiation. *Development* **124,** 381–389 (1997).

63. Thompson, M. a *et al*. The cloche and spadetail genes differentially affect hematopoiesis and vasculogenesis. *Dev*. *Biol*. **197,** 248–269 (1998).

64. Fuhrmann, S., Levine, E. M. & Reh, T. A. Extraocular mesenchyme patterns the optic vesicle during early eye development in the embryonic chick. **4609,** 4599–4609 (2000).